JEMMME (Journal of Energy, Mechanical, Material, and Manufacturing Engineering)
Vol. 7, No. 2, 2022

ISSN 2541-6332 | e-ISSN 2548-4281
Journal homepage: http://ejournal.umm.ac.id/index.php/JEMMME

A CFD analysis of NACA 0015 airfoil as a horizontal stabilizer with gap length variations

Gunawan Nugroho[a], Herman Sasongko[b], Mohammad Adenan[c], Sarwono[d], Heru Mirmanto[e]
[a, c, d] Department of Engineering Physics, Institut Teknologi Sepuluh Nopember
Kampus ITS Sukolilo-Surabaya 60111, Indonesia

[b] Department of Mechanical Engineering, Institut Teknologi Sepuluh Nopember
Kampus ITS Sukolilo-Surabaya 60111, Indonesia

[e] Department of Industrial Mechanical Engineering, Institut Teknologi Sepuluh Nopember
Kampus ITS Sukolilo-Surabaya 60111, Indonesia
e-mail: gunawan@ep.its.ac.id

Abstract

The horizontal stabilizer is an important device which stabilizes in the longitudinal direction is an important device for aviation. It also controls the pitching nose through the variation of elevator deflection angle. This work is to relate the lift coefficient with elevator deflection angle. The applied horizontal stabilizer is a plain flap with a gap length of 1.75%, 2% and 2.25% w.r.t. chord length. Results show that higher elevator deflection angle increases lift coefficient. For the 2-degree angle of attack and 20 degrees of elevator deflection angle, the lift coefficient is 0.93 (gap length 1.75%). Moreover, the lift coefficient is 1.83 for 10-degree horizontal stabilizer (gap length 2%).

Keywords*: elevator deflection angle; horizontal stabilizer; lift coefficient; plain flap*

1. INTRODUCTION

The stability components of vertical, lateral, and longitudinal directions are the most important in plane stability control. The yaw motion is controlled by rudder in vertical direction. The pitching motion is managed by elevator in lateral direction and the rolling motion is controlled in longitudinal direction. Different airfoil types are implemented for achieving the goal of stabilizing motions. Especially for the horizontal stabilizer, some aeroplanes use symmetrical airfoil with NACA 64A012 and NACA 0012 (1,2). In the case of longitudinal stabilizer, the elevator is installed as a controlled fuselage at the back of horizontal stabilizer. The aeroplane nose will move downward if the elevator is downturned. The elevator is also synchronized to both move up and down. The deflection angles vary by 5°, 10°, 15°, 20°, 25° and 30° which depend on their types (3–5). Flow at end wall region becomes more complex because of this phenomenon because it is different from two-dimensional separation theory at mid span. Flow around end wall contain secondary flow span wise toward wall in different intensities. Ones develop theory based on experimental data and numerical calculation and it is concluded that it is due to boundary layer flat plate interaction (6,7). Flow will experience friction from flat plate and face adverse pressure gradient as a result of obstacle/appendage/airfoil. At this instant it resembles the two-dimensional flow separation theory, but the consequences are much more different.

Then it is concluded that the entire complexity of flow around the end wall takes place in the wake region. Such was the case; it can be stated that the entire phenomena caused by pressure distribution at end wall because the incoming kinetic energy which represented by velocity have damaged/separated. In more practical point, it is a potential loss because wake region is characterized by constant pressure distribution.

Three-dimensional flow wake also contains horseshoe vortex which becomes a blockage of main flow then both angle of attack and velocity vector will also be deflected. Experimental curve of cascade airfoil shows that end wall region occupies highest total pressure loss (8) and highest entropy increase also. Even in axial compressor, the blockage is such that large that results blade to blade flow and compressor will stall suddenly. There are many other aspects of three-dimensional flow that have been explored, as a comparable study states that total circulation in wake around tip region is identified approximately 40% times bound circulation near tip. This work analyzes and performs the CFD simulation of the relation of elevator deflection angles with gap length variations.

2. METHODS

This research begins with the design of NACA 0015 geometry which is based on the airfoil coordinate data as depicted in figure 1.

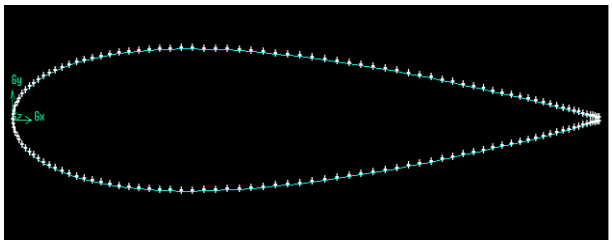

Figure 1. NACA 0015 geometry

Table 1. Mesh size at boundary layer

No	Physical Domain	Mesh size
1	First layer	0,0331 mm
2	Growth factor	1,3
3	Row	40
4	Transition pattern	1:1

Specifying the far field domain by installing the airfoil in the middle as shown in figure 2 (9).

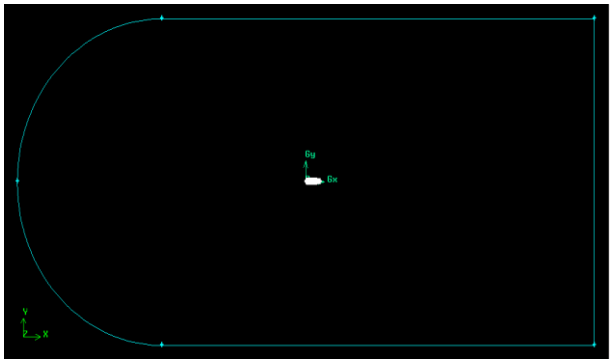

Figure 2. Fairfield domain

The next step is to mesh the computational domains which the mesh density of the sensitive and physically important are more than surrounding.

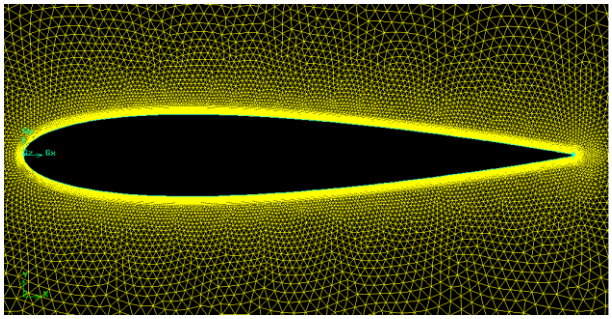

Figure 3. Meshing boundary layer

In this case, the gradual meshing process is applied and becomes denser in the airfoil surface as shown in Figure 4.

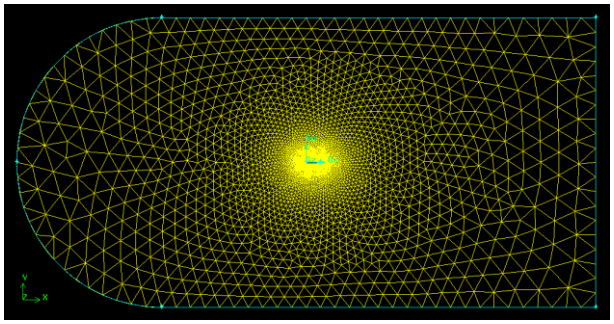

Figure 4. Meshing of all domains

The step now is to implement boundary conditions.

Table 3. Boundary conditions

Surface	Boundary conditions	Initial boundary
Airfoils	*Wall*	Airfoils
Upper wall	*Pressure Fairfield*	
Bottom wall	*Pressure Fairfield*	Pff
Front wall	*Pressure Fairfield*	
Back wall	*Pressure Fairfield*	

3. RESULT AND DISCUSSION

Firstly, airfoil is tested against NACA report No. 586, which the experimental data without the elevator. The airfoil is tested at Re 2.27x106 and velocity of 21.03 m/s. The geometry is valid if the deviation is less than or equal 5% and then the gap length variations are performed. The simulations show that the deviation is large at angle of attack of 14° until 20°. This is due to the massive flow separation behind the airfoil which then decreases the lift coefficient and stalls occur. On the other hand, the deviation with smaller angle of attack is less than 5% and verified (10). Hence, the boundary conditions and mesh size can be applied for further investigations (11).

Table 4. Verification

AoA	CL (Report)	CL (Simulation)	Deviation (%)
0	*0*	0	-
2	*0,22*	0,21	0,10
4	*0,444*	0,43	0,77
6	*0,66*	0,64	1,56
8	*0,88*	0,85	2,81
10	*1,04*	1,05	0,67

12	*1,16*	1,20	3,23
14	*1,19*	1,39	16,38
16	*1,13*	1,51	33,15
18	*1,05*	1,52	44,69
20	*0,99*	1,20	21,05

The next step is to divide NACA 0015 into two parts which are horizontal stabilizer at front and elevator in the back. The elevator length is 35% of chord length as depicted in figure 5.

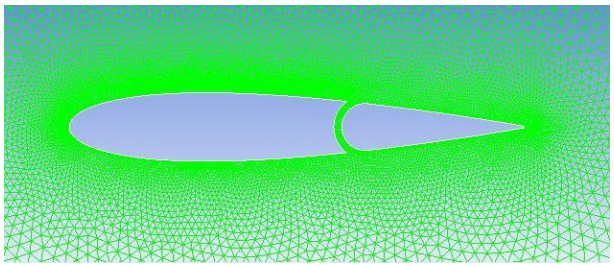

Figure 5. The dividing of NACA 0015

In this research the gap length is varied by 1,75%, 2% dan 2,25% of chord length and the results of angle of attack 2° are depicted in figure 6.

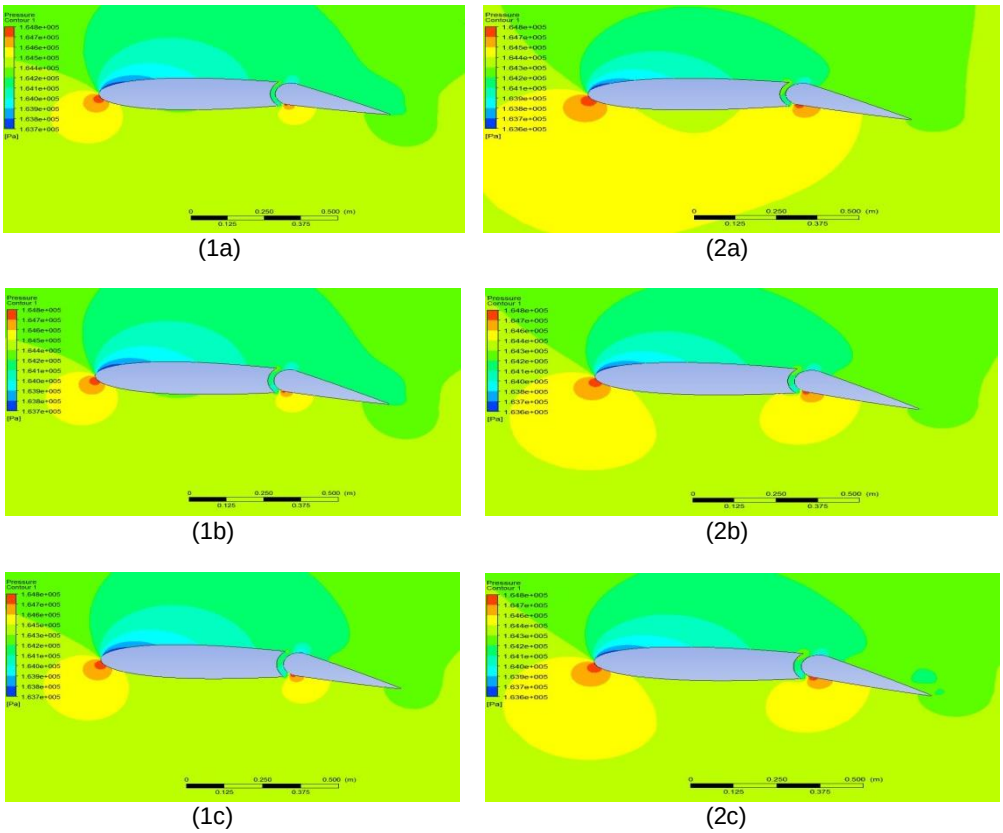

(1a) (2a)

(1b) (2b)

(1c) (2c)

Figure 6. Pressure contour of 2° AoA (1) DF 16°; (2) DF 20° and gap length (a) 1.75%; (b) 2%; (c) 2.25%

a) Elevator Deflection of 16°

At the gap length of 1,75% and 2% the pressure shows that the smallest pressure area is shifted toward the elevator trailing edge. This will increase the friction coefficient,

as the friction coefficient of gap length 1,75% and 2% is 0.8 which is smaller than the case with 2,25% of gap length.

b) Elevator Deflection of 20°

In the upper surface area, the small pressure is due to the flow interactions with the lower surface. The flow from the lower surface entering the gap will interact with the upper surface flow which then increases the velocity. Also, the interaction will form the small wake which then increases adverse pressure gradient in the elevator upper surface. The small-scale wake area of 1,75% gap length is relatively smaller than the case of 2% and 2,25% gap length.

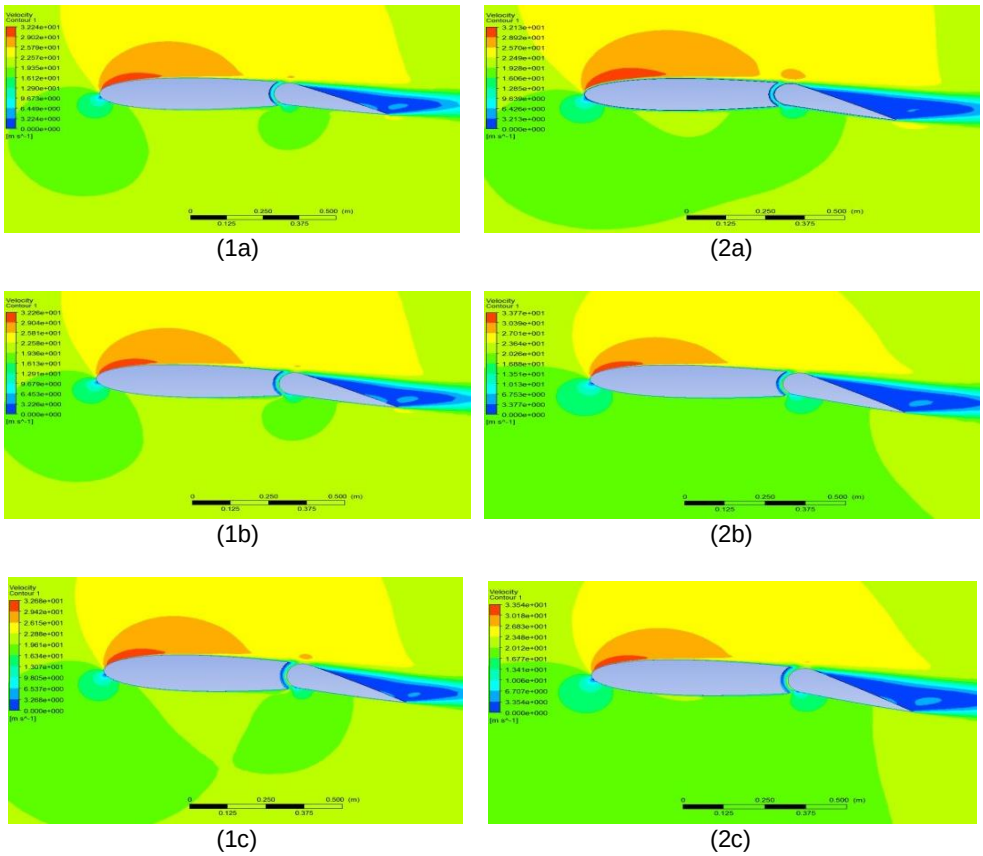

(1a) (2a)

(1b) (2b)

(1c) (2c)

Figure 7. Velocity contour of 2° AoA (1) DF 16°; (2) DF 20° with the gap length of (a) 1.75%; (b) 2%; (c) 2.25%

a) Elevator Deflection of 16°

It is shown that there are stagnation points at the horizontal stabilizer leding edge for each gap length. After the stagnation point the flow accelerates and then experiencing adverse pressure gradient in the elevator. The change of airfoil geometry due to elevator deflection angle will distribute the flow. The small-scale wake at the upper surface receives more momentum from the lower surface through the gap and part of the flow is still able to pass the elevator upper surface.

The lift coefficient of 2.25% gap length is higher due to the reverse flow at the elevator upper surface is smaller than the case of 1.75% and 2% gap length. Also, flow acceleration occurs in the elevator leading edge from the gradual contour change from green to yellow, which shows that the flow is more in the 2.25% gap length.

b) Elevator Deflection of 20°

The highest lift coefficient is from the gap length of 1.75% due to bubble separation at the horizontal stabilizer lower surface. In this case the flow tends toward elevator leading edge come from the gap. This is shown by the occurrence of the small-scale

wake at the elevator leading edge and different from the case of 2% and 2.25%, which the flow is more under the lower surface of horizontal stabilizer. Also, the elevator separation points of 2% and 2.25% gap length are closer to the leading edge compared to 1.75% gap length. The next step is to explore the case of angle of attack 10° which is depicted by the pressure contour as in the following.

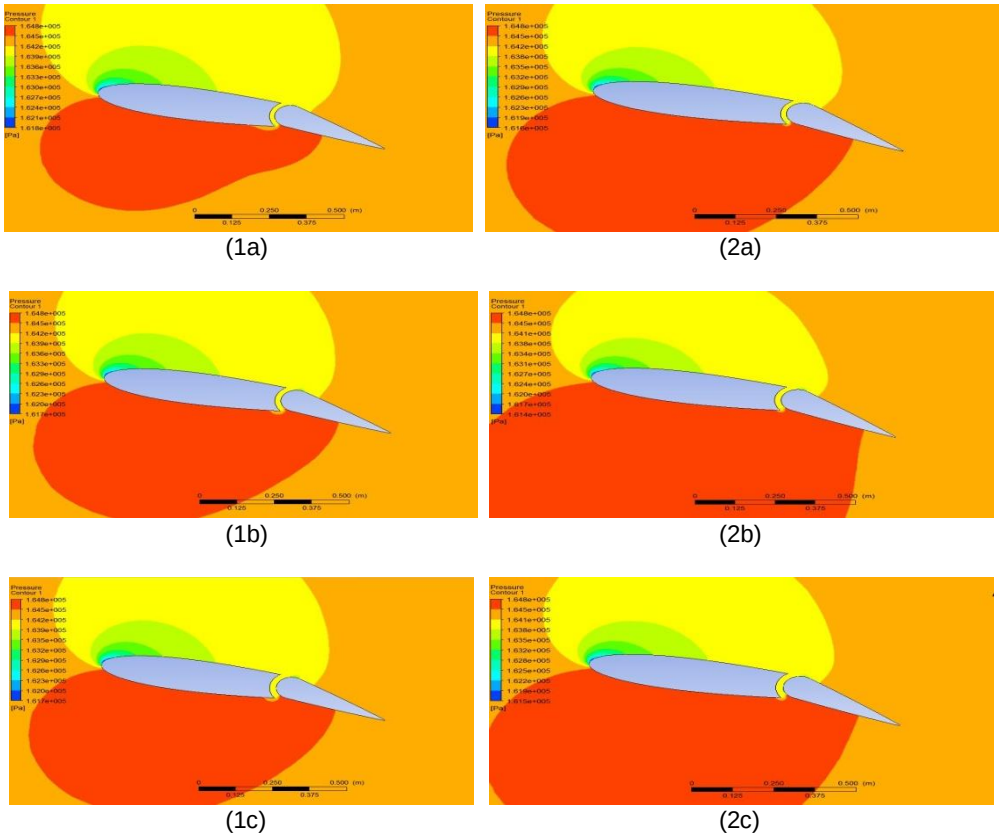

(1a) (2a)

(1b) (2b)

(1c) (2c)

Figure 8. Pressure contour of 10° AoA (1) DF 16°; (2) DF 20° with gap length of (a) 1.75%; (b) 2%; (c) 2.25%

a) Elevator Deflection of 16°

At the lower surface of horizontal stabilizer trailing edge with 1,75% gap length, the bigger pressure area is detected compared to the case of 2% and 2.25% gap length. This is due to the smaller gap length which then will block the flow at the lower trailing edge of horizontal stabilizer. The case of 2% and 2.25% gap length are the flow tends to pass the gap. Hence, the lift coefficient of 1.75% gap length is the smallest. The pressure difference in the case of 2% and 2.25% gap length is not significant and the difference of the lift coefficient is small, i.e., 1.64 for 2% gap length and 1.66 for 2.25% gap length. However, there is a difference in pressure at the elevator lower surface. The higher pressure of 2.25% gap length at the elevator lower surface tends toward trailing edge compared to 2% gap length. This will increase the lift coefficient for the 2.25% gap length.

b) Elevator Deflection of 20°

For the case of 20° deflection, the lower lift coefficient is detected for 1,75% gap length, i.e., 1.68. It is also investigated that even if the blockage is smaller, the higher-pressure area is smaller at the lower surface than the case of 2% and 2.25% gap length. It is also supplemented by the result that the largest higher-pressure area is at the gap length of 2% which resulted in the highest lift coefficient. On the other hand, it is also observed that the maximum pressure is closer to the trailing edge.

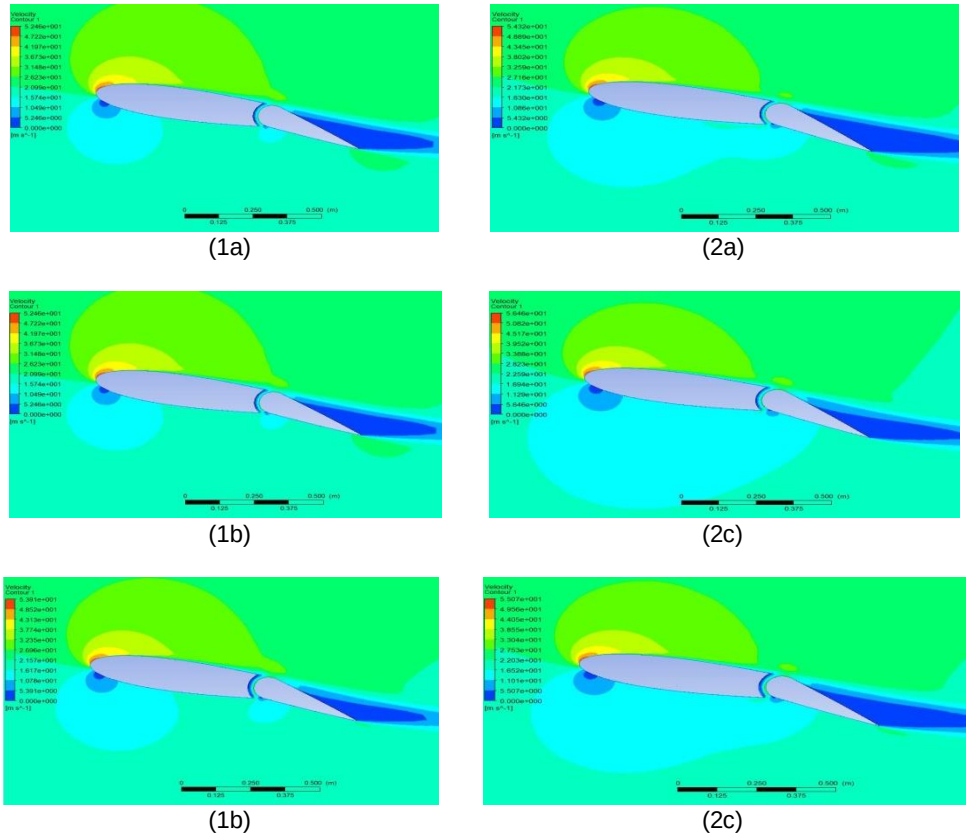

Figure 9. Velocity contour of 10° AoA (1) DF 16°; (2) DF 20° with gap length of (a) 1,75%; (b) 2%; (c) 2,25%

a) Elevator Deflection of 16°

The velocity contour shows two stagnation points at the leading edge of horizontal stabilizer and elevator. This is due to the higher angle of attack such that the freestream attaching two leading edges. This phenomenon produces higher lift coefficient because the flow accelerates on both sides. The velocity distribution from the three gap length variations shows a similar pattern, but different in separation points. The separation point of gap length 2,25% tends toward elevator trailing edge and generates highest lift coefficient of 1,66.

b) Elevator Deflection of 20°

The velocity profile shows the velocity of 16.52 m/s dominating at the lower side. The velocity pattern is similar with the 16° deflection and similar for three gap length variations. The difference is on the occurrence of small-scale wake at the elevator upper surface. The highest lift coefficient is produced in the 2% gap length which is 1.83. This is supported by the delayed separation that is closer to the elevator trailing edge. On the other hand, the flow tends to move through the gap and increases the velocity at the upper surface.

4. CONCLUSION

The flow around horizontal stabilizer and elevator is analyzed in this research. CFD simulation is implemented with the pre-evaluation of the airfoil data of NACA 0015. Results show that the lift coefficient is higher than without the elevator. It is observed that increasing gap length is not always followed by higher lift coefficient. It is also found that the gap variation is related with the elevator deflection angle for producing higher lift coefficient.

REFERENCES

1. Perkins HD, Wilson J, Raymer DP. An evaluation of performance metrics for high efficiency tube-and-wing aircraft entering service in 2030 to 2035. Ohio; 2011.
2. Lefebvre AM, Zha G. Design of High Wing Loading Compact Electric Airplane Utilizing Co-Flow Jet Flow Control. In: 53rd AIAA Aerospace Sciences Meeting. Reston, Virginia: American Institute of Aeronautics and Astronautics; 2015. doi: https://doi.org/10.2514/6.2015-0772
3. Obert E. Aerodynamic Design of Transport Aircraft. Delft; 2009.
4. Lee S, Bragg MB. Experimental Investigation of Simulated Large-Droplet Ice Shapes on Airfoil Aerodynamics. J Aircr. 1999 Sep;36(5):844–50. doi: https://doi.org/10.2514/2.2518
5. Bolonkin A, Gilyard GB. Estimated benefits of variable-geometry wing camber control for transport aircraft. California; 1999.
6. Lampart P. Investigation of endwall flows and losses in axial turbines. J Theor Appl Mech. 2009;47(2):321–42.
7. Pullan G. Secondary Flows and Loss Caused by Blade Row Interaction in a Turbine Stage. J Turbomach. 2006 Jul 1;128(3):484–91. doi: https://doi.org/10.1115/1.2182001
8. Cui J, Tucker P. Numerical Study of Purge and Secondary Flows in a Low-Pressure Turbine. J Turbomach. 2017 Feb 1;139(2). doi: https://doi.org/10.1115/1.4034684
9. Jacobs E, Sherman A. Airfoil section characteristics as affected by variations of the Reynolds number. J Franklin Inst. 1937 Nov;224(5):670. doi: 10.1016/s0016-0032(37)90818-4
10. Anderson JD. Computational fluid dynamics: Basics with applications. Singapore: McGraw-Hill Book Companies, Inc.; 2005.
11. T. Ramadhan, Analisa Performansi Flap Pesawat N-2xx Terhadap Perubahan Gap Dan Overlap Di PT. Dirgantara Indonesia. Surabaya: Institut Teknologi Sepuluh Nopember, 2016.